Estimating Faults in Nonlinear DC Microgrids with Constant Power Loads: A Dual-Extended Kalman Filter Approach

Navid Vafamand, and Mohammad Mehdi Arefi
School of Electrical and Computer Engineering, Shiraz University,
Shiraz, Iran
{n.vafamand, arefi}@shirazu.ac.ir

Miadreza Shafie-khah
School of Technology and Innovations, University of Vaasa,
Vaasa, Finland
mshafiek@univaasa.fi

João P. S. Catalão
Faculty of Engineering of the University of Porto and INESC TEC,
Porto, Portugal
catalao@fe.up.pt

2021 IEEE International Conference on Environment and Electrical Engineering and 2021 IEEE Industrial and Commercial Power Systems Europe (EEEIC / I&CPS Europe) | 978-1-6654-3613-7/21/$31.00 ©2021 IEEE | DOI: 10.1109/EEEIC/ICPSEurope51590.2021.9584736

***Abstract*—This article investigates the problem of detecting and estimating actuator fault in direct current microgrids (DC MGs) with linear and nonlinear constant power loads (CPLs). The actuator fault is modeled by using an additive term in the state-space and highly influences the system response if it is not compensated. An advanced dual-extended Kalman filter (dual-EKF) is proposed to estimate the system states and the accruing actuator fault. Though the presented approach offers a systematic procedure to divide the augmented state vector into two parts and these parts can be estimated in parallel. Thereby, the online computational burden is reduced as it can be implemented by two processes in parallel. The proposed approach does not require restrictive assumptions on the system matrices and is robust against stochastic Gaussian noises. The proposed approach is applied on a practical faulty DC MG benchmark connected to a CPL; and, the results are compared with other state-of-the-art methods from the computational burden and estimation accuracy points of view.**

Keywords—DC microgrid, Constant power load, Actuator Fault, Extended Kalman Filter, Estimation.

I. INTRODUCTION

Direct current (DC) and alternating current (AC) microgrids (MGs) are an effective solution to integrate distributed loads and renewable energy sources [1]. For recent power utilities involving DC wind turbine, fuel cells, and photovoltaics and DC electronic loads, it is wise to consider the DC MGs [1]. Thanks to power electronic advances, DC Mgs are now widely feeding tightly controlled loads that are inherently nonlinear and act as constant power loads (CPLs). The main issue associated with CPLs is that possess a destabilizing negative incremental resistance behavior. The CPL stability issue has been attracting many attentions and different linear and nonlinear control strategies have been presented [2]–[4]. However, in none of those references the issue of fault detection and fault tolerant control is investigated.

Indeed, reviewing the state-of-the-art methods reveals that the faulty operation of islanded DC MGs with CPLs has been rarely investigated. Nevertheless, occurring rigorous faults not only degrades the DC MG efficiency and reliability but also damages the MG connected elements if they are not detected and treated accordingly. In [5], the influence of several faults on a DC MG with multiple CPLs is investigated, and a fault-tolerant control (FTC) method was suggested to the closed-loop system robust against faults. However, that approach suggests the FTC for each CPL connected to the DC MG.

J.P.S. Catalão acknowledges the support by FEDER funds through COMPETE 2020 and by Portuguese funds through FCT, under POCI-01-0145-FEDER-029803 (02/SAICT/2017).

By increasing the number of CPLs, that approach is not cost-effective. In [6], the effect of sensor fault on a typical DC MG was investigated. However, the other classes of faults were ignored. A robust controller and monitoring technique was developed in [7] to alleviate the consequence of occurring faults. Though, the faults were not reconstructed. In [8], the actuator and sensor faults were detected by developing a robust linear observer. However, the detected faults were not estimated. Also, the detection performance degrades when the system contains nonlinear elements. In [9], both the actuator and sensor faults were detected and reconstructed. In that approach, a sliding mode observer was suggested.

However, to design the observer gains, several assumptions on the ranks of the system were required. In parallel to the abovementioned attempts dealing with faults, several estimation methods have been presented in MGs to estimate the states, including estimating the' flux of rotor in motors [10], the state-of-charge in energy storage systems [11], and the currents in DC MGs [12]. However, in none of those approaches, the issue of occurring faults in the power system has been not investigated. This is the main motivation for this work. This paper focuses on the problem of detecting and estimating actuator faults in DC MGs with linear loads and CPLs. A model-based dual-extended Kalman filter (dual-EKF) is presented through which the system states and actuator fault are evaluated and constructed in parallel. The developed approach extends the results of the conventional extended Kalman filter (EKF) such that it not only capable of dealing with faulty systems but also requires almost the same computational time burden as the EKF.

The main advantages of the proposed approach over the state-of-the-art method [9] are that I) it does not expose restrictive assumptions on the system matrices and II) is robust against stochastic Gaussian noises. To show the merits of the developed dual-EKF approach, it is tested on a DC MG benchmark that feeds CPLs and resistive loads. The comparative results are also presented to verify that the computational burden, implementation complexity, and estimation accuracy of the proposed approach outperforms the conventional version of nonlinear Kalman filters.

II. FAULTY DC MC WITH CPLS

A typical DC MG involves some power generators, storage, and loads. These loads can be resistive or constant power, as shown in Fig. 1.

The difference between the resistive loads and CPLs is appearing power electronic load converters. The CPLs are commonly integrated into DC MGs at the input point of the load converter by assuming the converters are ideal or consume constant power.

978-1-6654-3613-7/21/$31.00 ©2021 IEEE

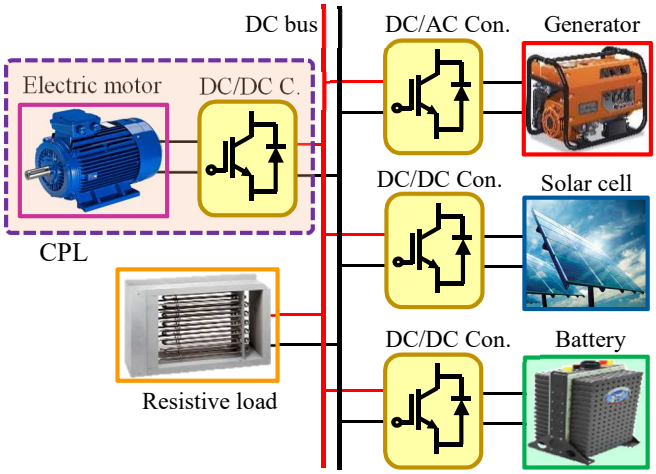

Fig. 1. Power system illustration of a DC MG.

The simplified electric schematic of the DC MG is shown in Fig. 2, where comprises a DC source, a controllable DC/DC converter, $\mathcal{J}$ CPLs, and $\mathcal{K}$ RLs. Since the resistive loads R_s for $s = 1, \dots, \mathcal{J}$ and CPLs P_{CPL_s} for $s = 1, \dots, \mathcal{K}$ are in parallel, their equivalent resistive load (i.e. R) and CPL (i.e. P) are computed as follows:

$$R = \left(R_1^{-1} + \cdots + R_{\mathcal{J}}^{-1}\right)^{-1} \tag{1}$$

$$P = P_{CPL_1} + \cdots + P_{CPL_{\mathcal{K}}} \tag{2}$$

The DC/DC buck converter is described by an averaged-model and by the duty cycle $u \in \{0,1\}$. The system is subjected to actuator and sensor faults. Merging the nonlinear DC MG system with actuator and sensor faults results that:

$$\begin{cases} C\dfrac{dv_C}{dt} = i_L - \dfrac{v_C}{R} - \dfrac{P}{v_C} \\ L\dfrac{di_L}{dt} = V_e u - v_C + V_e f_a \\ y = v_c \end{cases} \tag{3}$$

where the v_c and i_L are voltage and current of the capacitor and inductor, specified by the capacitance and inductance C and L, respectively. V_e is the source voltage. Furthermore, the f_a is the actuator additive fault. As can be seen in (3), the actuator fault appears in the control input channel. This fault affects the control action and degrades the DC MG performance.

The state-space representation of the dynamics (3) is as follows:

$$\begin{cases} \dot{x}_1 = \dfrac{1}{C}x_2 - \dfrac{x_1}{RC} - \dfrac{P}{Cx_1} \\ \dot{x}_2 = \dfrac{V_e}{L}u - \dfrac{1}{L}x_1 + \dfrac{V_e}{L}f_a \\ y = x_1 \end{cases} \tag{4}$$

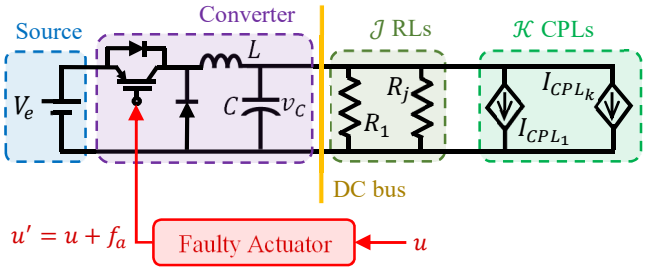

Fig. 2. A basic diagram of the DC MG with $\mathcal{K}$ CPLs, $\mathcal{J}$ resistive loads, and actuator fault f_a.

The goal is to estimate the actuator fault as well as the state vector based on the available voltage measurement. This is done by presenting an improved nonlinear dual-Kalman filter.

III. Proposed Nonlinear State and Fault Estimator

A. Modifying the state-space representation

Estimating information of (4) has two main challenges due to appearing the actuator fault and the nonlinear term $1/x_1$. Initially, to tackle with the actuator fault f_a, it are considered as an augmented state. On the other hand, since its time derivative is unknown, it is considered that

$$\dot{f}_a = 0 \tag{5}$$

It is worthy to note that, if there is any pre-knowledge of f_a, the dynamics (5) can be updated. Now, by defining the augmented vector $X = [x_1 \;\; x_2 \;\; x_3]^T = [x^T \;\; f_a]^T$ and reminding (4) and (5) one has:

$$\begin{cases} \dot{X} = F(X) + G(X)u \\ Y = H(X) \end{cases} \tag{6}$$

where

$$F(X) = \begin{bmatrix} F_1(X) \\ F_2(X) \\ F_3(X) \end{bmatrix} = \begin{bmatrix} \dfrac{1}{C}x_2 - \dfrac{x_1}{RC} - \dfrac{P}{Cx_1} \\ -\dfrac{1}{L}x_1 + \dfrac{V_e}{L}x_3 \\ 0 \end{bmatrix}; \quad G(X) = \begin{bmatrix} 0 \\ \dfrac{V_e}{L} \\ 0 \end{bmatrix}, H(X) = x_1 \tag{7}$$

Now, the continuous-time representation (6) is discretized by the Euler approach with the sample time T_s and subjected to system and measurement noises v and w. Thereby

$$\begin{cases} X(k+1) = \bar{F}\big(X(k)\big) + \bar{G}\big(X(k)\big)u(k) + v(k) \\ Y(k) = H\big(X(k)\big) + w(k) \end{cases} \tag{8}$$

where

$$\bar{F}\big(X(k)\big) = X(k) + T_s F\big(X(k)\big)$$
$$\bar{G}\big(X(k)\big) = T_s G\big(X(k)\big)$$

B. Dual-Extended Kalman Filter

The main objective is to estimate the state vector X_k in the presence of noise. Although is feasible to use the conventional EKF approach, the overall computational burden increases due to the fact that the dimension of the augmented state vector increases. Besides, it is not needed to estimate the faults, whenever they do not appear. Thereby, the conventional EKF is modified such that it estimates the actual system states and faults separately and simultaneously. Consequently, the part of faults estimation can be sopped, whenever it is needed. Additionally, the overall computational burden decreases by splitting the augmented states $X(k)$ into two vectors.

The rationale behind the dual-EKF is to define two vectors a and b, as $X(k) = [a^T(k) \;\; b^T(k)]^T$ and $a(k) = [x_1(k) \;\; x_2(k)]^T$ and $b(k) = [f_a(k)]^T$. Then, both the state and fault vectors are estimated by two modified EKFs which operate in parallel.

The EKF algorithm is a nonlinear extension version of the linear KF, which uses the Jacobian matrix of the dynamics (8).

For the ease of summarizing the dual-EKF algorithm, the dynamics (8) is represented by its Jacobian matrix, as follows:

$$\begin{cases}\begin{bmatrix}a(k+1)\\ b(k+1)\end{bmatrix}=\begin{bmatrix}\Psi_{aa}(k) & \Psi_{ab}(k)\\ \Psi_{ba}(k) & \Psi_{bb}(k)\end{bmatrix}\begin{bmatrix}a(k)\\ b(k)\end{bmatrix}+\\ \qquad\qquad\qquad\qquad\begin{bmatrix}B_a\\ B_b\end{bmatrix}u(k)+\begin{bmatrix}v_a(k)\\ v_b(k)\end{bmatrix}\\ y(k)=C[a^T(k)\quad b^T(k)]^T+w(k)\end{cases}\tag{9}$$

where $v(k)=[v_a^T(k),v_b^T(k)]^T$ and $v(k)$ are the system and measurement noise vectors, characterized by Gaussian function $\mathcal{g}$ with mean vector and variance matrix, as follows:

$$\begin{bmatrix}v_a(k)\\ v_b(k)\end{bmatrix}\sim\mathcal{g}\left(0,\begin{bmatrix}Q_a(k) & 0\\ 0 & Q_b(k)\end{bmatrix}\right)\tag{10}$$

$$w(k)\sim\mathcal{g}(0,R(k))\tag{11}$$

Also,

$$\Psi_{ab}(k)=\left[\begin{matrix}\frac{\partial\bar{F}_1(X)}{\partial b}\\ \frac{\partial\bar{F}_2(X)}{\partial b}\end{matrix}\right]\Bigg|_{X=X(\boldsymbol{k})}=\begin{bmatrix}0\\ \frac{T_sV_e}{L}\end{bmatrix}\tag{12}$$

$$\begin{aligned}\Psi_{aa}(k)&=\left[\begin{matrix}\frac{\partial\bar{F}_1(X)}{\partial a}\\ \frac{\partial\bar{F}_2(X)}{\partial a}\end{matrix}\right]\Bigg|_{X=X(k)}\\ &=\begin{bmatrix}1+\frac{-T_s}{RC}+\frac{PT_s}{Cx_1^2(k)} & \frac{T_s}{C}\\ -\frac{T_s}{L} & 1\end{bmatrix}\end{aligned}\tag{13}$$

$$\Psi_{ba}(k)=\left[\frac{\partial F_3(X)}{\partial a}\right]\Big|_{X=X(k)}=0\tag{14}$$

$$\Psi_{bb}(k)=\left[\begin{matrix}\frac{\partial\bar{F}_3(X)}{\partial b}\\ \frac{\partial\bar{F}_4(X)}{\partial b}\end{matrix}\right]\Bigg|_{X=X(\boldsymbol{k})}=\begin{bmatrix}1 & 0\\ 0 & 1\end{bmatrix}\tag{15}$$

$$B_a=\begin{bmatrix}0 & \frac{T_sV_e}{L}\end{bmatrix}^T;\ B_b=0\tag{16}$$

$$C_a=[1\quad 0];\ C_b=0\tag{17}$$

As can be seen in (17), the system output only contains the vector $a(k)$. This is mandatory in the proposed dual-EKF approach, so that the EKF of $a(k)$ can be estimated independent to the EKF filter of $b(k)$, the later filter is stopped. Based on the dual estimation idea [13]–[15], in the following, two nonlinear KFs will be developed for the system (9):

- Initial conditions for state filter

$$\begin{cases}\hat{a}^+(0)=E\{a(0)\}\\ P_a^+(0)=E\{(a(0)-\hat{a}^+(0))(a(0)-\hat{a}^+(0))^T\}\end{cases}\tag{18}$$

- Initial conditions for fault filter

$$\begin{cases}\hat{b}^+(0)=E\{b(0)\}\\ P_b^+(0)=E\left\{\left(b(0)-\hat{b}^+(0)\right)\left(b(0)-\hat{b}^+(0)\right)^T\right\}\end{cases}\tag{19}$$

where $\hat{a}^+(.)$ and $\hat{b}^+(.)$ are the estimation of the vectors a and b; and $P_a^+(.)$ and $P_b^+(.)$ covariance matrices of the estimation errors. For $k=1,2,\ldots$ the following recursive algorithms are performed:

- State filter time update

$$\begin{cases}\hat{a}^-(k)=\Psi_{aa}(k)\hat{a}^+(k-1)\\ P_a^-(k)=\Psi_{aa}(k)P_a^+(k-1)\Psi_{aa}^T(k)+Q_a(k-1)\end{cases}\tag{20}$$

- Fault filter time update

$$\begin{cases}\hat{b}^-(k)=\Psi_{bb}(k)\hat{b}^+(k-1)\\ P_b^-(k)=\Psi_{bb}(k)P_b^+(k-1)\Psi_{bb}^T(k)+Q_b(k-1)\end{cases}\tag{21}$$

- State filter measurement update

$$\begin{cases}K_a(k)=P_a^-(k)C_a^T(C_aP_a^-(k)C_a^T+R(k))^{-1}\\ \hat{a}^+(k)=\hat{a}^-(k)+K_a(k)(y(k)-C_a\hat{a}_k^-)\\ P_a^+(k)=(I-K_a(k)C_a)P_a^-(k)\end{cases}\tag{22}$$

- Fault filter measurement update

$$\begin{cases}K_b(k)=P_a^-(k)C_w^T(k)(C_w(k)P_b^-(k)C_w^T(k)+R(k))\\ \hat{b}^+(k)=\hat{b}^-(k)+K_b(k)(y(k)-C_a\hat{a}_k^-)\\ P_b^+(k)=(I-K_b(k)C_w(k))P_b^-(k)\end{cases}\tag{23}$$

where the matrix $C_w(k)$ will be updated as follows:

$$C_w(k)=C\left.\frac{\partial\hat{a}^+(k)}{\partial b}\right|_{b=\hat{b}^-(k)}\tag{24}$$

and, the approximation of the derivative term is computed recursively, as follows:

$$\begin{cases}\frac{\partial\hat{a}^+(k)}{\partial b}=(I-K_a(k)C_a)\frac{\partial\hat{a}^-(k)}{\partial b}\\ \frac{\partial\hat{a}^-(k+1)}{\partial b}=\Psi_{aa}(k)\frac{\partial\hat{a}^+(k)}{\partial b}+\Psi_{ab}(k)\end{cases}\tag{25}$$

Reminding the iterative algorithm given in (20)-(25), the flowchart of the dual-EKF algorithm is summarized in Fig. 3.

Remark 1 (Advantages of the proposed approach): Although several control approaches have been developed for model-based control and monitoring of nonlinear DC MGs with CPLs, few approaches considered the issue of faults in DC MGs. Also, few approaches have been considered in the literature. Comparing with these approaches, the proposed approach, has some advantages summarized as follows: I) it does not need any restrictive assumption, II) it offers a low online computational burden and can be implemented by two processors, III) it is robust against uncertainties, which is not the case in the existing results. The overall system implementation is shown in Fig. 4. As can be seen in Fig. 4, the voltage of the MG bus is measured continuously with the sampling time T_s. Then, the dual-EKF is performed to estimate the states and faults. This information can be then considered for different actions including monitoring, controlling, and repairing or replacing the converter.

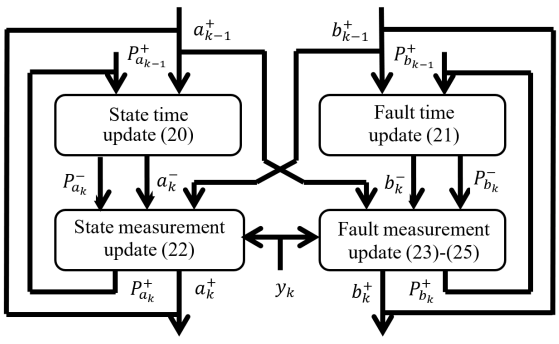

Fig. 3. Flowchart of the nonlinear dual-Kalman filter algorithm. (The index of notations in this figure shows the discrete-time instance).

IV. Simulation Results

The developed approach is applied the DC MG dynamics (3) with the parameters $R = 10\ (\Omega)$, $C = 500\ (\mu F)$, $L = 39.5\ (mH)$, $P = 300\ (W)$, $V_e = 200\ (V)$, and $u = 0.5$. Also, the sampling time is $T_s = 1\ (msec)$ and the measurement noise variance is 0.1. To show its merits, it is compared with conventional EKF in which the fault is not estimated. Two scenarios of fault-free and actuator fault are considered in the following.

Scenario 1 (Fault-free system): In this scenario, the effectiveness and computational burden of the proposed approach and the conventional EKF are compared. The closed-loop system states are presented in Fig. 5. Since the issue of designing a controller is not considered in this paper, the duty cycle is set as $u = 0.5$, and the DC MG bus voltage and current reach 100 (V) and 13 (A) in about 0.1 (sec).

The estimation errors of the system states are shown in Fig. 6, in which the blue and red lines resent the conventional EKF and the developed dual-EKF, respectively. As can be seen in Fig. 6, both approaches offer the same estimation accuracy for both the voltage and current of the DC MG. Comparing with the nominal values of the system states in Fig. 5, one infers that the Kalman filters robustly estimate the system states in Figs 6(a) and (b) in the presence of white noisy measurement.

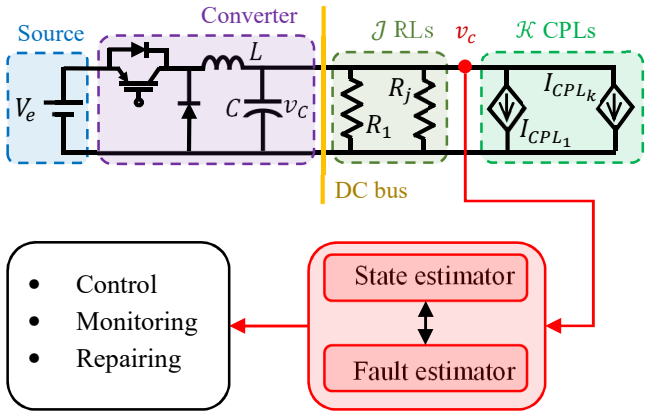

Fig. 4. The implementation of the dual-EKF for the DC MG.

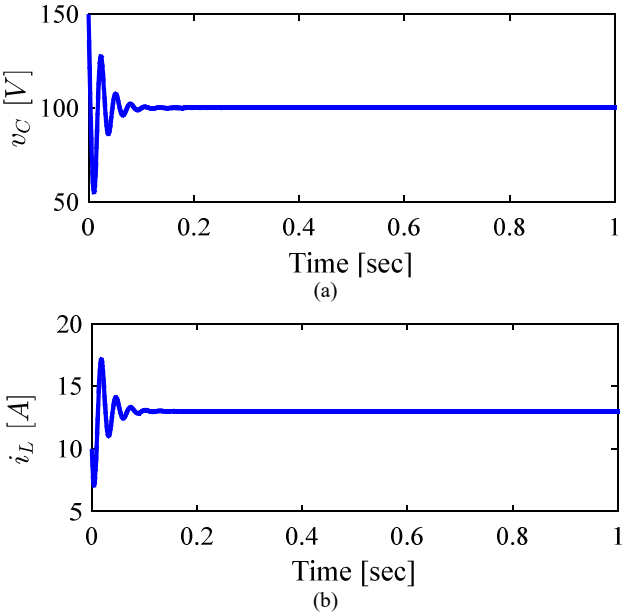

Fig. 5. The actual system states of Scenario 1: (a) $x_1 = v_C$, (b) $x_2 = i_L$.

Moreover, Fig. 6 (c) shows the estimation of the actuator fault for the dual-EKF approach. Due to noisy measurements, it estimates the zero actuator with the error amplitude of the order 0.002 with is neglectable by comparing with the amplitude of the applying duty cycle $u = 0.5$.

To have a better insight of computational burden and estimation accuracy of both estimators Table I is provided. The computational burdens are calculated as the mean value of each iteration of 100 simulations with different white noises via core-5 computer environment. The results reveal that the computational burdens of both approaches are almost the same. Additionally, the dual-EKF slightly needs more to perform the estimations. The difference is originated from the fact that the Dual-EKF needs to perform two state and actuator estimators, simultaneously.

The state and fault estimators require 11.4017 and 8.1267 milliseconds, respectively. If these estimators are implemented by two processors in parallel, then the overall computation burden would be 11.4017 milliseconds, which is the same as the conventional EKF time of 11.4012 milliseconds.

Additionally, the estimation error indices of Table I illustrate that the dual-EKF slightly outperforms the conventional EKF for the steady-state amplitude error and the norm 2 (, which is related to the energy) of the estimation error. Though, this small improvement may be spoiled if the system is resituated and with a different white noise signal.

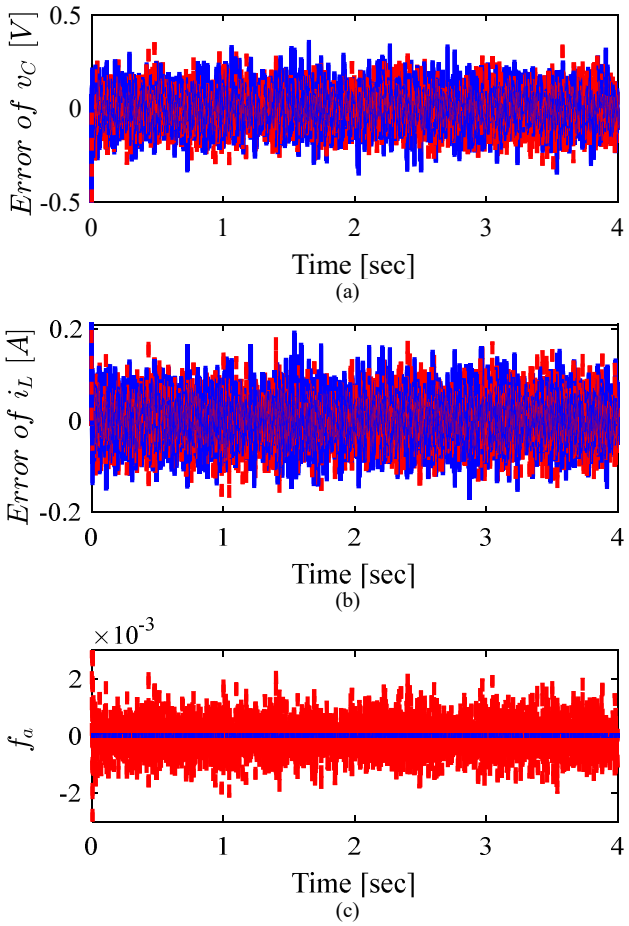

Fig. 6. Estimation error of Scenario 2 (Conventional EKF by the blue line and dual-EKF by the red line): (a) estimation of $x_1 = v_C$, (b) estimation of $x_2 = i_L$, (c) estimation of f_a.

TABLE I. PERFORMANCE COMPARISON OF TWO APPROACHES FOR SCENARIO 1.

	EKF	Dual-EKF
Mean of the computational burden	1.14×10^{-4}	1.95×10^{-4}
Norm 2 of the estimation error of v_c	21.0625	20.9638
The maximum steady-state error of v_c	0.3975	0.3987
Norm 2 of the estimation error of i_L	8.2180	8.0936
The maximum steady-state error of i_L	0.1940	0.1932

Scenario 2 (System with actuator fault): In this scenario, the accuracies of the proposed dual-EKF approach and the conventional EKF in the presence of actuator fault are evaluated. The actuator fault is assumed to be time-varying as $f_a = 0.2\sin(4/3\pi t)$. The systems states are influenced by the actuator fault and behave oscillatory, as shown in Fig. 7. As discussed before, the voltage regulator is not considered to keep the DC bus voltage constant.

The estimation errors of the system states and actuator fault are shown in Fig. 8. Fig. 8 reveals that the first state, v_c, is estimated accurately based on both approaches. The reason is that the noisy measured output is the voltage and therefore, both approaches only need to decompose the noise signal for the measurement. Though, the dual-EKF again offers better performance than conventional-EKF. However, the estimation of the second state, i_L is affected by the additive actuator fault. Since the conventional EKF cannot estimate the actuator fault, it does not provide an accurate estimation of i_L; and, its estimation involves an evolution of the fault f_a. However, the dual-EKF estimates the state x_2 more precisely. The minor error is produced, because the actuator fault is varying and its estimation has one step lag, as shown in Fig. 8. If the sampling time $T_s = 0.001\ (sec)$ decreases, the dual-EKF performance improves.

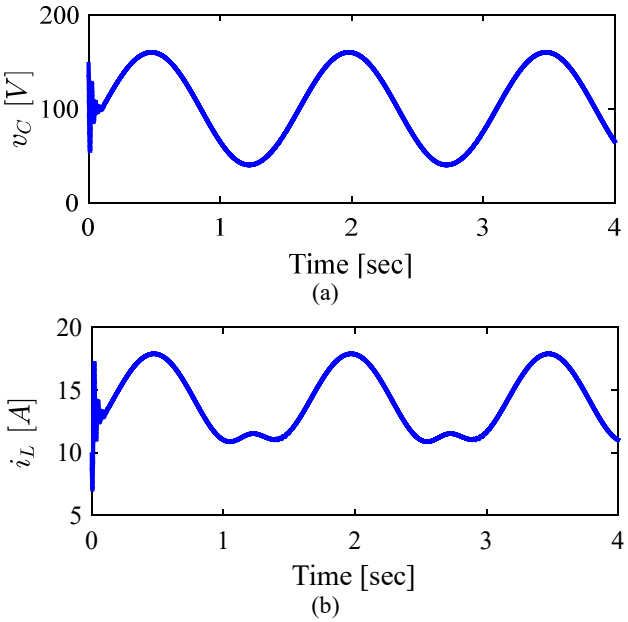

Fig. 7. The actual system states of Scenario 2: (a) $x_1 = v_c$, (b) $x_2 = i_L$.

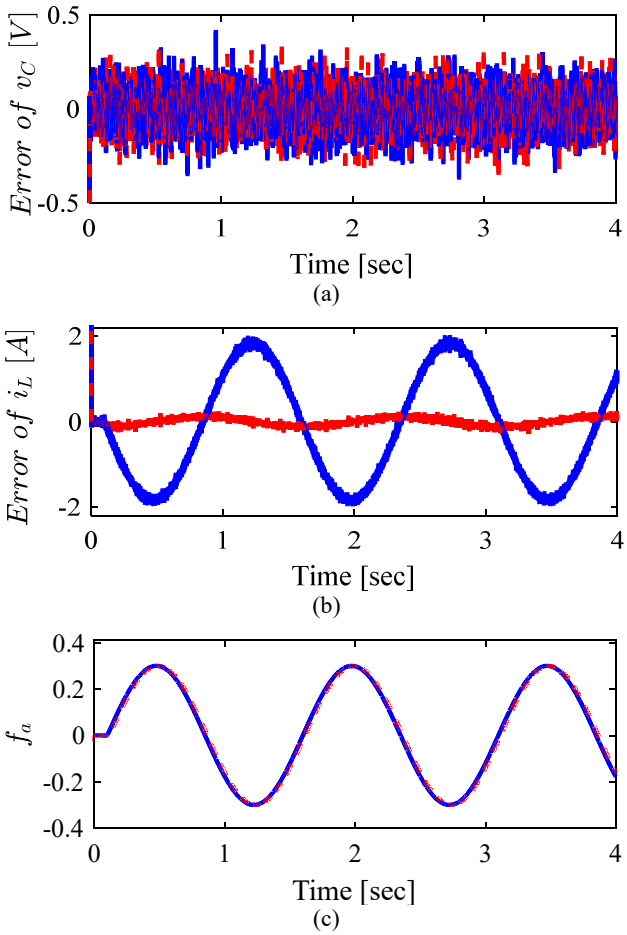

Fig. 6. Estimation error of Scenario 1 (Conventional EKF by the blue line and dual-EKF by the red line): (a) estimation of $x_1 = v_c$, (b) estimation of $x_2 = i_L$, (c) estimation of f_a.

V. CONCLUSION

In this article, the issue of state and actuator fault estimation for DC MGs with nonlinear dynamics was studied. It was assumed that the considered DC MG feeds linear resistive loads and nonlinear CPLs. A novel dual-EKF approach was suggested for the power system. This enhanced version dual-EKF combines two EKFs each estimates the system states or the actuator fault. It was shown that the state EKF can work indecent to the fault EKF. So, it is possible to use only one Kalman filter whenever the actuator fault does not happen. Or, each Kalman filter is implemented on a processor. The performance improvement of the dual-EKF over the conventional EKF is shown through numerical simulations and by scenarios of fault-free and fault-affected systems. The results showed that in the presence of actuator fault, the conventional EKF leads to poor accuracy. In comparison, the dual -EKF not only estimates the states and the fault accurately but also requires almost the same computational burden as the conventional EKF. For future work, considering system and sensor faults and incorporating the developed approach with the model predictive controller are suggested.

REFERENCES

[1] H. Bevrani, B. Francois, and T. Ise, *Microgrid Dynamics and Control*. Hoboken, NJ, USA: John Wiley & Sons, Inc., 2017.

[2] N. Vafamand, S. Yousefizadeh, M. H. Khooban, J. D. Bendtsen, and T. Dragicevic, "Adaptive TS Fuzzy-Based MPC for DC Microgrids with Dynamic CPLs: Nonlinear Power Observer Approach," *IEEE Syst. J.*, vol. 13, no. 3, pp. 3203–3210, 2018, doi: 10.1109/JSYST.2018.2880135.

[3] A. Vafamand, N. Vafamand, J. Zarei, R. Razavi-Far, and T. Dragicevic, "Intelligent Multi-objective NSBGA-II Control of Power Converters in DC Microgrids," *IEEE Trans. Ind. Electron.*, pp. 1–1, 2020, doi: 10.1109/TIE.2020.3029483.

[4] Q. Xu, N. Vafamand, L. Chen, T. Dragicevic, L. Xie, and F. Blaabjerg, "Review on Advanced Control Technologies for Bidirectional DC/DC Converters in DC Microgrids," *IEEE J. Emerg. Sel. Top. Power Electron.*, pp. 1–1, 2020, doi: 10.1109/JESTPE.2020.2978064.

[5] P. Magne, B. Nahid-Mobarakeh, and S. Pierfederici, "A design method for a fault-tolerant multi-agent stabilizing system for DC microgrids with Constant Power Loads," in *2012 IEEE Transportation Electrification Conference and Expo (ITEC)*, Dearborn, MI, USA, Jun. 2012, pp. 1–6, doi: 10.1109/ITEC.2012.6243469.

[6] S. Saha, T. K. Roy, M. A. Mahmud, M. E. Haque, and S. N. Islam, "Sensor fault and cyber attack resilient operation of DC microgrids," *Int. J. Electr. Power Energy Syst.*, vol. 99, pp. 540–554, Jul. 2018, doi: 10.1016/j.ijepes.2018.01.007.

[7] R. Todd and A. J. Forsyth, "DC-bus power quality for aircraft power systems during generator fault conditions," *IET Electr. Syst. Transp.*, vol. 1, no. 3, p. 126, 2011, doi: 10.1049/iet-est.2010.0056.

[8] A. Salimi, Y. Batmani, and H. Bevrani, "Model-Based Fault Detection in DC Microgrids," in *2019 Smart Grid Conference (SGC)*, Tehran, Iran, Dec. 2019, pp. 1–6, doi: 10.1109/SGC49328.2019.9056589.

[9] S. Asadi, N. Vafamand, M. Moallem, and T. Dragicevic, "Fault Reconstruction of Islanded Nonlinear DC Microgrids: An LPV-based Sliding Mode Observer Approach," *IEEE J. Emerg. Sel. Top. Power Electron.*, pp. 1–1, 2020, doi: 10.1109/JESTPE.2020.3043491.

[10] M. Barut, R. Demir, E. Zerdali, and R. Inan, "Real-Time Implementation of Bi Input-Extended Kalman Filter-Based Estimator for Speed-Sensorless Control of Induction Motors," *IEEE Trans. Ind. Electron.*, vol. 59, no. 11, pp. 4197–4206, Nov. 2012, doi: 10.1109/TIE.2011.2178209.

[11] R. Xiong, H. He, F. Sun, and K. Zhao, "Evaluation on State of Charge Estimation of Batteries with Adaptive Extended Kalman Filter by Experiment Approach," *IEEE Trans. Veh. Technol.*, vol. 62, no. 1, pp. 108–117, Jan. 2013, doi: 10.1109/TVT.2012.2222684.

[12] M. A. Kardan *et al.*, "Improved Stabilization of Nonlinear DC Microgrids: Cubature Kalman Filter Approach," *IEEE Trans. Ind. Appl.*, vol. 54, no. 5, pp. 5104–5112, Sep. 2018, doi: 10.1109/TIA.2018.2848959.

[13] N. Vafamand, M. M. Arefi, and A. Khayatian, "Nonlinear system identification based on Takagi-Sugeno fuzzy modeling and unscented Kalman filter," *ISA Trans.*, vol. 74, pp. 134–143, Feb. 2018, doi: 10.1016/j.isatra.2018.02.005.

[14] E. A. Wan and A. T. Nelson, "Dual Kalman filtering methods for nonlinear prediction, smoothing, and estimation," *Adv. Neural Inf. Process. Syst.*, vol. 9, pp. 793–799, 1997.

[15] H. Khodadadi and H. Jazayeri-Rad, "Applying a dual extended Kalman filter for the nonlinear state and parameter estimations of a continuous stirred tank reactor," *Comput. Chem. Eng.*, vol. 35, pp. 2426–2436, 2011.